Atmos. Chem. Phys., 14, 3211–3230, 2014
www.atmos-chem-phys.net/14/3211/2014/
doi:10.5194/acp-14-3211-2014

Atmospheric Chemistry and Physics Open Access

Numerical simulation of "an American haboob"

A. Vukovic[1,2], M. Vujadinovic[1,2], G. Pejanovic[2], J. Andric[3], M. R. Kumjian[4], V. Djurdjevic[2,5], M. Dacic[2], A. K. Prasad[6], H. M. El-Askary[6,7], B. C. Paris[8], S. Petkovic[2], S. Nickovic[9,10], and W. A. Sprigg[11,12]

[1]Faculty of Agriculture, University of Belgrade, Serbia
[2]South East European Virtual Climate Change Center, RHMSS, Belgrade, Serbia
[3]Rosenstiel School of Marine and Atmospheric Science, University of Miami, Miami, FL, USA
[4]National Center for Atmospheric Research, Boulder, CO, USA
[5]Institute of Meteorology, Faculty of Physics, University of Belgrade, Belgrade, Serbia
[6]School of Earth and Environmental Sciences, Chapman University, Orange, CA, USA
[7]Department of Environmental Sciences, Alexandria University, Moharem Bek, Alexandria, Egypt
[8]Arizona Department of Environmental Quality, Phoenix, AZ, USA
[9]World Meteorological Organization, Geneva, Switzerland
[10]Institute of Physics, Belgrade, Serbia
[11]Institute for Atmospheric Physics, The University of Arizona, Tucson, AZ, USA
[12]WMO Pan-American Center for SDS-WAS, Chapman University, Orange, CA, USA

Correspondence to: A. Vukovic (pazisadana@gmail.com)

Received: 27 June 2013 – Published in Atmos. Chem. Phys. Discuss.: 10 October 2013
Revised: 28 January 2014 – Accepted: 18 February 2014 – Published: 2 April 2014

Abstract. A dust storm of fearful proportions hit Phoenix in the early evening hours of 5 July 2011. This storm, an American haboob, was predicted hours in advance because numerical, land–atmosphere modeling, computing power and remote sensing of dust events have improved greatly over the past decade. High-resolution numerical models are required for accurate simulation of the small scales of the haboob process, with high velocity surface winds produced by strong convection and severe downbursts. Dust productive areas in this region consist mainly of agricultural fields, with soil surfaces disturbed by plowing and tracks of land in the high Sonoran Desert laid barren by ongoing draught.

Model simulation of the 5 July 2011 dust storm uses the coupled atmospheric-dust model NMME–DREAM (Nonhydrostatic Mesoscale Model on E grid, Janjic et al., 2001; Dust REgional Atmospheric Model, Nickovic et al., 2001; Pérez et al., 2006) with 4 km horizontal resolution. A mask of the potentially dust productive regions is obtained from the land cover and the normalized difference vegetation index (NDVI) data from the Moderate Resolution Imaging Spectroradiometer (MODIS). The scope of this paper is validation of the dust model performance, and not use of the model as a tool to investigate mechanisms related to the storm. Results demonstrate the potential technical capacity and availability of the relevant data to build an operational system for dust storm forecasting as a part of a warning system. Model results are compared with radar and other satellite-based images and surface meteorological and PM_{10} observations. The atmospheric model successfully hindcasted the position of the front in space and time, with about 1 h late arrival in Phoenix. The dust model predicted the rapid uptake of dust and high values of dust concentration in the ensuing storm. South of Phoenix, over the closest source regions ($\sim$25 km), the model PM_{10} surface dust concentration reached $\sim$2500 µg m^{-3}, but underestimated the values measured by the PM_{10} stations within the city. Model results are also validated by the MODIS aerosol optical depth (AOD), employing deep blue (DB) algorithms for aerosol loadings. Model validation included Cloud-Aerosol Lidar and Infrared Pathfinder Satellite Observation (CALIPSO), equipped with the lidar instrument, to disclose the vertical structure of dust aerosols as well as aerosol subtypes. Promising results encourage further research and application of high-resolution modeling and satellite-based remote sensing to warn of approaching severe dust events and reduce risks for safety and health.

Published by Copernicus Publications on behalf of the European Geosciences Union.

1 Introduction

Particular sandstorms, called haboobs ("habb" – to blow), are very frequent events in Sudan (Sutton, 1925). The Sudan haboob appears mostly in the rainy season in the afternoon hours, followed by thunderstorms and wind speeds of 50–70 km h^{-1}, carrying dust to heights over 1000 m and dust wall diameters to 30–40 km. With the development of aviation it was possible to collect more information about these sandstorms. In his following paper, Sutton (1931) presents more data on such events. They are characterized by a sharp fall in temperature and a sudden strong wind often followed by rain. The principal cause for such events appears to be related to a current of relatively cold air undercutting warm air. Similar events have been recognized in India and Iraq. Pilots have reported great instability and convection in the region of such sandstorms. In the following decades, knowledge and theory about haboob formation, processes and characteristics have developed. Freeman (1952) has shown that the haboob can last for more than 6 h with a peak intensity lasting between 30 min to 1 h. Average haboob duration is about 3 h. These and other characteristics reported by Sutton (1931), such as fluctuation in air pressure, fall in air temperature, and rise of relative humidity are also confirmed. A decrease in the air temperature in severe cases can be as great as 15 °C, with the maximum wind speed twice the haboob's speed of advance (Lawson, 1971). The shape of the leading edge is not one large arc, but consists of several "lobes" (Lawson, 1971). Idso (1973) and Idso et al. (1972) noticed dust storms with characteristics similar to those in Sudan also appear in the arid southwestern United States.

"An American haboob" is the title of a paper by Idso et al. (1972), which, for the first time, recognized a Sudanese sandstorm called haboob over American soil. A haboob is generally caused by downdrafts from thunderstorms that develop over mountain regions in southern Arizona. Thunderstorms that develop southeast of Tucson usually continue to move through the Santa Cruz Valley and arrive in Phoenix in the period 17:00–21:00 local time (LT). Other storms, not as severe, generally arrive between 15:00 and 17:00 LT. Dust storms in most cases are followed by thunder and rain, within approximately 2 h. The severe dust storm appears to take the shape of a squall line, composed of multiple cells that probably contribute to its own downdraft pattern and can intensify on its path through the Valley. The leading edge can be 100 mi (∼160 km) wide with a wall of dust reaching 8000 ft (∼2400 m). The authors describe a classic haboob that occurred on 16 July 1971: a massive dust storm hit Phoenix in the evening hours, spawned from thunderstorms that developed over southern Arizona near Tucson. Severe downdrafts dropped near-surface temperature, raised humidity and pressure, and forced high velocity winds over the dry soil of Santa Cruz Valley, picking up dust from the dry, hot soil. Using available measurements and photographs of the event they reconstructed the shape and path of the storm. It was clear that it consisted of merged macro-lobes, which were composed of smaller micro-lobes. This was a good example of describing similarities with haboobs in Sudan. Idso et al. (1972) estimated that about half of the major dust storms that occur in the southwest US are haboobs (2–3 in a year). The event that happened decades later, on 5 July 2011, the subject of this paper, had the same general characteristics.

A general lack of observations of the haboob environment prior to its formation, during its life span and after its demise inhibits full understanding of the haboob process. Hales (1975) used satellite and radar data, along with ground measurements from synoptic stations, to produce detailed explanations of a severe southwest US desert thunderstorm case. Gillette et al. (1978) presented measurements from the ground and aircraft measurements aloft, of dust particle size distribution during dust storm events over erodible sites (bare and agricultural) in Texas, Oklahoma, New Mexico and Arizona; they noticed a log-normal distribution with modes around 6 µm diameter. Dust samples collected at 1m above the ground have a bimodal particle size distribution: 1–30 µm diameter range and 30–100 µm range. Aircraft measurements over and far from erodible areas showed a single mode 1–20 (or 30) µm. These studies found that only a small portion of the dust produced by wind erosion is carried to higher altitudes (2–9 km) over long distances. They also noticed that desert soil erodes at a lesser rate than agricultural areas. The dust particle size distribution during the dust storm event in Texas is also described in Chen and Fryrear (2002).

Wilkerson (1991) highlighted that haboobs received considerable attention in the previous 10 years due to several aircraft crashes related to micro-bursts (Fujita, 1986), a common feature generating haboobs. Because of the small scale of a micro-burst it is difficult to forecast. A mesoscale high-pressure area and strong winds are created from cool sinking air and heavy rain under a thunderstorm. It is common that most or all of the rain evaporates before reaching the ground because the surrounding area is very dry, cooling the air further and accelerating the downdraft. Upon meeting the ground, strong downdrafts become high-velocity horizontal wind, pushing out from the cloud downdraft region. These horizontal winds continue through the desert, picking up dust. Small solenoidal circulations are formed at the leading edge. An horizontal vortex forms within the cool air at the nose of the frontal area that faces warm air, which then contributes greatly to uptake of large amounts of dust (Fujita, 1986). The dust cloud may reach 10–14 000 ft (3000–4300 m) (Idso, 1976). Visibility falls rapidly inside the haboob (Lawson, 1971). Most dust particles within these storms are 10–50 µm (Lawson, 1971), but larger particles (several mm) are also carried along (Foster, 1969), although settling rapidly. The haboob travels fast and the air clears quickly as dust is advected out of the area.

Characteristics of the density currents, which generate dust propagation, are summarized in Solomos et al. (2012). They showed that the area of the maximum dust productivity

is related to the increased turbulence (reverse flow) near the surface behind the leading edge. More information on density currents can be found in Knippertz et al. (2007), Emmel et al. (2010), Knippertz and Todd (2012).

Pauley et al. (1996) described a dust storm on 29 November 1991 that caused a pileup on Interstate 5 in California, US, involving 164 vehicles. They reported that dust uptake came from surrounding agricultural areas that were left unplanted after being plowed, before the rainy season began; disturbing a soil surface makes it more susceptible to dust generation (Gillete et al., 1980). Pauley et al. (1996) also noted that in these agricultural regions dust is present often enough that the US Environmental Protection Agency (EPA) is proposing sanctions for San Joaquin Valley growers for not attending the standard for PM_{10} (particulate matter of 10 micrometers or less). It should also be noted that drought conditions had prevailed in that area for 6 years.

Numerical models for simulation/forecast of the dust cycle are generally inter-compared over the large geographic domains (Uno et al., 2006; Todd et al., 2008). These studies showed a large variability in model performance, up to one order of magnitude. Typical resolutions of regional dust models are several tens of kilometers, and global model resolutions are ∼100 km or coarser. It is not general practice to use dust models with higher resolutions. However, Sundram et al. (2004) describes simulations of dust storm events over central and eastern Washington using a CALMET/CALGRID model and a new dust emission module EMIT-PM, driven by MM5, on 4 km resolution. Considering the complexity of the events, these experiments produced excellent results. The model performed best for large, strong dust storms, but did not simulate smaller storms or dust plumes. They noted that in order to simulate individual dust events it is necessary to use high-resolution dust models and to introduce agricultural areas as dust productive sources. Extensive studies over the Sahara region also highlight the relevance in use of high-resolution numerical models for simulation of such events (e.g. Knippertz et al., 2009; Marsham et al., 2011; Johnson et al., 2011; Solomos et al., 2012; Tegen et al., 2013; Schepanski et al. 2013).

On 5 July 2011, a dust storm having all the characteristics of an haboob formed in the area around Tucson, Arizona, and moved north toward Phoenix through the Santa Cruz Valley. High wind gusts picked up dust particles along the way, creating a high (> 5000 ft), wide (1 mile) and dense (visibility zero) wall of dust that hit Phoenix in the early evening hours. Available ground and radar measurements, National Weather Service Forecast Office and news media reports, amateur photos and videos of the storm, showed that this event was much like the one described by Idso et al. (1972). All this information indicated that for successful numerical simulation of the event, the model must represent convective activity and active dust sources very well. This dust storm was created by the high surface winds generated from strong downbursts of cold air. High wind velocity over the bare and dry land created favorable conditions for intense dust uptake and transport. In our numerical simulation of this event we would expect to face several significant problems: definition of dust sources; ability of the model to simulate location, timing and strength of the downburst and high velocity winds; and ability of the model to produce high dust concentrations in a very short time. We used the atmospheric model NMME (Nonhydrostatic Mesoscale Model on E grid, Janjic et al., 2001) coupled with the dust model DREAM (Dust REgional Atmospheric Model, Nickovic et al., 2001; Pérez et al., 2006). Model resolution was 4 km. The model is informed of the potential dust-productive area from the NDVI data closest to the date of the haboob under study obtained from MODIS. In forecast operations, the dust sources are refreshed for model ingestion every 16 days.

2 Phoenix dust storm on 5 July 2011

The North American Monsoon is a climatological feature over a large part of North America and of the southwest US in particular (Douglas et al., 1993; Adams and Comrie, 1997). Spring and summer warming of Mexico and the southwest US, followed by shifts of wind and atmospheric pressure patterns during summer, bring moisture into the hot dry environment from, primarily, the Gulf of California and eastern Pacific at low altitude, and upper level moisture transported by easterly winds from the Gulf of Mexico. Additional moisture may invade the arid southwest from the southern planes of the US that are usually wet and green during early summer months. Much of western North America is affected by a quickly developing, distinct rainy season due to this combination of wind pattern and moisture inflow. Dual rainfall patterns are present in the US southwest. The first one occurs from December through March; the second pattern from July through September. The summer monsoon brings surges of wet tropical air and frequent but localized violent thunderstorms, arriving in the southwest US in early July. The largest portion of the July and August precipitation over the southwestern US averages over 50 and 70 mm, respectively (Hu and Feng, 2002). However, in 2011 much of the southern plains had been under long-term drought and the pattern of the monsoon setup early, although inflow of deep moisture from Mexico was lacking. It became a summer of extreme heat, drought and dust storms. Records show 33 days with temperatures higher than 110 °F (43 °C) in Phoenix, well above the normal of 18 days (source news media reports, Vukovic et al., 2011).

The National Weather Service (NWS) forecast office in its report on the 5 July dust storm (http://www.wrh.noaa.gov/psr/pns/2011/July/DustStorm.php) provides an explanation and description of this event. The southwest US was affected badly by ongoing drought. This area received less than 50 % normal precipitation since the end of the previous summer, leaving the ground dry. The US Drought Monitor

placed the area between Tucson and Phoenix in "moderate" to "extreme" drought category. During the North American Monsoon, dust storms are a common phenomenon across the Sonoran Desert. According to NCDC (National Climatic Data Center) storm data, in the past 10 years over 100 significant dust storm events were reported across Arizona; the Phoenix area averages one to three large dust storms per year (Raman and Arellano, 2013). During the 2011 summer there were six in this region. The most severe of these occurred on 5 July. The NWS Forecast office estimated the dust reached a peak height of at least 5000–6000 ft (1500–1800 m), with an areal coverage on the leading edge stretching nearly 100 miles (160 km). The main dust cloud traveled at least 150 miles (240 km). Blowing dust reduced visibility in Phoenix to zero. At about 19:00 MST (02:00 UTC) the dust wall hit the far southeast part of Phoenix and moved through the city during the next two hours. The cause for this event was the development of severe thunderstorms in southern Arizona that produced downburst winds, enhanced along the storm path between Tucson and Phoenix because of topography, a drop in elevation of 460 m. Strong outflow winds continued north, crossing over very dry areas. This dust storm halted traffic on roads and highways. Air traffic into and out of Phoenix Sky Harbor International Airport was stopped for 45 min. This storm was classified as an haboob. NWS/Phoenix reported the formation of the cold-pool atmospheric circulation north of Phoenix, which merged with the haboob's cold air (Raman and Arellano, 2013). Cold-pool formation is related to the thunderstorm outflows that reached the ground and produced severe downburst.

3 Model description and dust sources

For successful numerical simulation and forecast of the 5 July 2011 and similar events, it is necessary to have a high-resolution numerical model (Vukovic et al., 2011; Raman and Arellano, 2013). Haboobs are characterized by intense vertical mixing, which requires that non-hydrostatic mode models should be used. Sources of the dust in the southwest US are mainly agricultural fields scattered over the region, highly dust productive after plowing. While it appears to be a major dust source, an undisturbed desert landscape acquires a hard, low-eroding surface over time. Therefore, a detailed map of the potential dust sources is required as the input information for a dust model.

For our numerical simulation of the 5 July 2011 haboob we used the coupled regional atmospheric-dust model NMME–DREAM. It is driven in-line by the NOAA/NCEP (National Centers for Environmental Prediction) atmospheric numerical weather prediction model NMME. DREAM is designed to simulate the atmospheric cycle of mineral dust aerosol (Nickovic et al., 2001, 2004; Nickovic, 2002, 2003, 2005; Pérez et al., 2006; Xie et al., 2008; Pejanovic et al., 2010; Nickovic et al., 2012). The NMME–DREAM solves the Euler-type partial differential nonlinear equation for dust mass continuity. The concentration equation simulates all major processes of the atmospheric dust cycle: dust emission, turbulent diffusion, vertical and horizontal advection, lateral diffusion, and wet and dry deposition. Dust particle size distribution is described by eight bins with effective radii of 0.15, 0.25, 0.45, 0.78, 1.3, 2.2, 3.8, and 7.1 µm, according to Tegen and Lacis (1996). The main difference between DREAM and other dust models is that the dust transport parameterization in DREAM includes a viscous sublayer between the surface and the lowest model layer (Janjic, 1994), since there is a physical similarity between mass–heat–momentum exchanges over surfaces such as ocean with that of mobilized dust particle over desert surfaces (Chamberlain, 1983; Segal, 1990). This parameterizes the turbulent transfer of dust into the lowest model layer accounting for different turbulent regimes (laminar, transient and turbulent mixing), using the simulated surface dust concentration as the lower boundary. Parameterization of the wet removal is done with a parameterization method for wet deposition involving rainfall rate and washout ratio (Nickovic et al, 2001). DREAM has demonstrated its capabilities in a number of validation studies (e.g. Pérez et al., 2006; Balis et al., 2006; Jiménez-Guerrero et al., 2008; Todd et al., 2008) using data from observation networks such as the European Lidar Network EARLINET and the AERONET/PHOTONS sun photometer network. The model has been validated and tested against measurements at source regions for SAMUM-I (Haustein et al., 2009) and BODEX research field campaigns (Todd et al., 2008). Dust transport models used to simulate events such as the one analysed in this paper should include transport of the larger particles even though these larger particles settle down fast; many populated areas (cities and roads) are close to the source regions. For this study, sizes larger than PM_{10} were not included because we did not want to change the model from its version used in this region for many test cases and because only PM_{10} measurements were available for model verification. Any modification of the model would also require extensive testing before being applied on single event.

DREAM provides operational dust forecasts in the SEEVCCC/RHMSS (South East European Virtual Climate Change Center, Republic Hydrometeorological Service of Serbia) as part of the World Meteorological Organization Sand and Dust Storm Warning Advisory and Assessment System (WMO SDS-WAS), and is validated on a daily basis. It and predecessor versions have been applied to the Southwest US (Yin et al., 2005; Morain et al., 2007, 2009; Sprigg et al., 2008; Estes et al., 2009; Yin and Sprigg, 2010; Sprigg et al., 2012). Herein we report on the NMME–DREAM numerical simulation of the haboob on 5 July 2011 in Phoenix, Arizona. Model horizontal resolution was 1/40 °(3.75 km hereafter in the text will be approximated with 4 km) with 60 vertical levels. Choice of horizontal resolution is based on the currently operational NOAA/NCEP forecast resolution

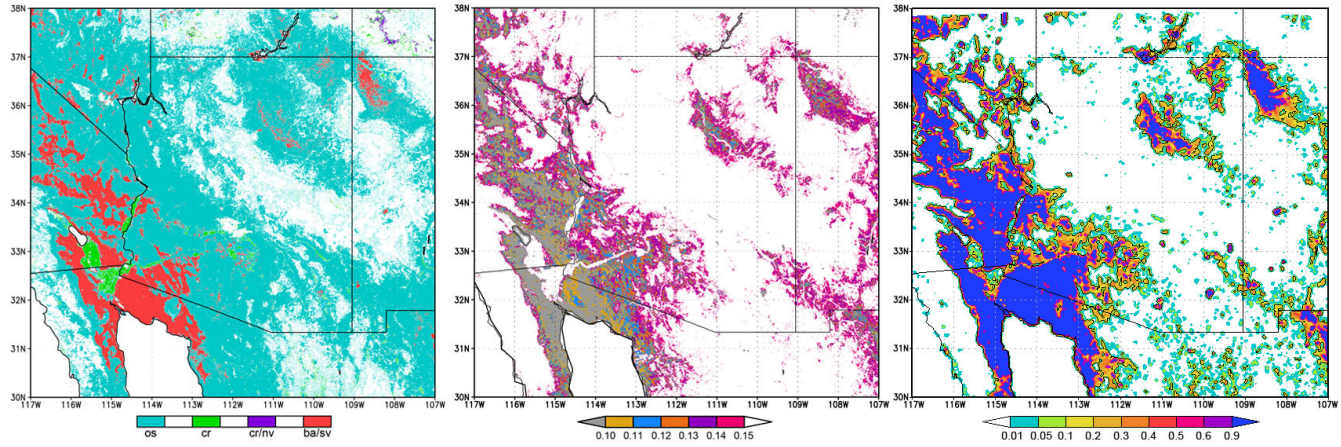

Fig. 1. MODIS land cover types: open shrubland – os, cropland – cr, cropland/native vegetation – cr/nv, barren/sparsely vegetated – ba/sv (left); NDVI (middle); mask of potentially dust productive areas on model resolution (right).

for this region (west-central US domain). High spatial resolution permits use of explicit convection, which is applied in model runs presented in this paper. Use of explicit convection, rather than a parameterization scheme, produces strong model downdraft and thereby more dust mobilization (Sprigg et al., 2012). Our model domain is 105° W–119° W, and 28° N–38° N. Forecast start time was 12:00 UTC 5 July 2011, and forecast is done for 24 h, with output data on 1 h interval. Model has cold start, with no dust in the initial field. In this case use of cold start can be considered valid based on observations of the storm and precursor meteorological conditions. The entire development of the dust storm was covered in the model simulation and no relevant airborne dust was observed prior to model start-up. This approach is not valid in all cases, and operational forecasting should begin with a warm star,(i.e. atmospheric dust should be inherited from the previous dust forecast). Initial and boundary conditions are downscaled from the ECMWF forecast data, which are on 16 km resolution every 3 h. Since the input global fields are from the forecast, and not the analysis field, we can consider NMME–DREAM results as a prediction or forecast of the event.

Specification of dust sources implies mapping of the areas that are dust productive under favorable weather conditions. The simplest approach is the application of only the land cover data (Nickovic et al. 2001; Walker et al. 2009), selecting the land cover types that are barren and arid. Another approach is to assume that dust productive regions are the ones that have long-term average of precipitation lower than some assigned threshold (Claquin et al., 1999). More precise selection of the dust productive regions can be done by adding the preferential dust sources related to topographic depressions containing sediments in paleolake and riverine beds (Ginoux et al., 2001; Prospero et al., 2002; Tegen et al., 2002; Zender et al., 2003). The first step is to find areas without vegetation. Second, to define areas inside barren regions with fine soil texture favorable for wind erosion. Usually, dust model simulations are performed over large areas that are generally barren but require additional information on the preferential dust sources (e.g. Sahara). In the southwest US, the structure of the dust sources is different. Because of high seasonal variability of the bare land areas related to agricultural fields, the main problem is to define precise locations without vegetation. These areas vary from year to year, also depending on the amount of precipitation. This issue was studied within NASA (National Aeronautics and Space Administration) sponsored projects PHAiRS (Public Health Applications in Remote Sensing) and ENPHASYS (ENvironmental Public Health Application SYStems). In PHAiRS (Morain et al., 2007, 2009; Sprigg et al., 2008), the dust mask derived from USGS land cover types in DREAM (Nickovic, 2005) was replaced with the one based on MODIS Land Cover Type Product (MCD12Q1). It considered only barren or sparsely vegetated areas. However, some dust events were not properly simulated when dust sources from agricultural areas were ignored during the non-vegetated season. Ensuing projects, ENPHASYS and "Airborne Dust Models: A Tool in Environmental Health Tracking" (Yin and Sprigg, 2010; Sprigg et al., 2012) included cropland without vegetation as a potential dust source using a NDVI layer from MODIS MOD13A2 data. This dust mask was updated every 16 days, which is the interval of availability for MOD13A2 data. The threshold for the NDVI of the cropland land cover type when it can be considered dust productive was found to be 0.25. Because of the highly heterogeneous nature of dust sources in the southwest US, we use horizontal model resolution less than 10 km. Lee et al. (2009) showed that dust events over these regions could be formed from the numerous dust plumes emitted from scattered, point-like sources that merge into a wide dust veil downwind. Raman and Arellano (2013), studying the same July 2011 haboob, also highlighted the importance of defining the dust sources: even simulations with

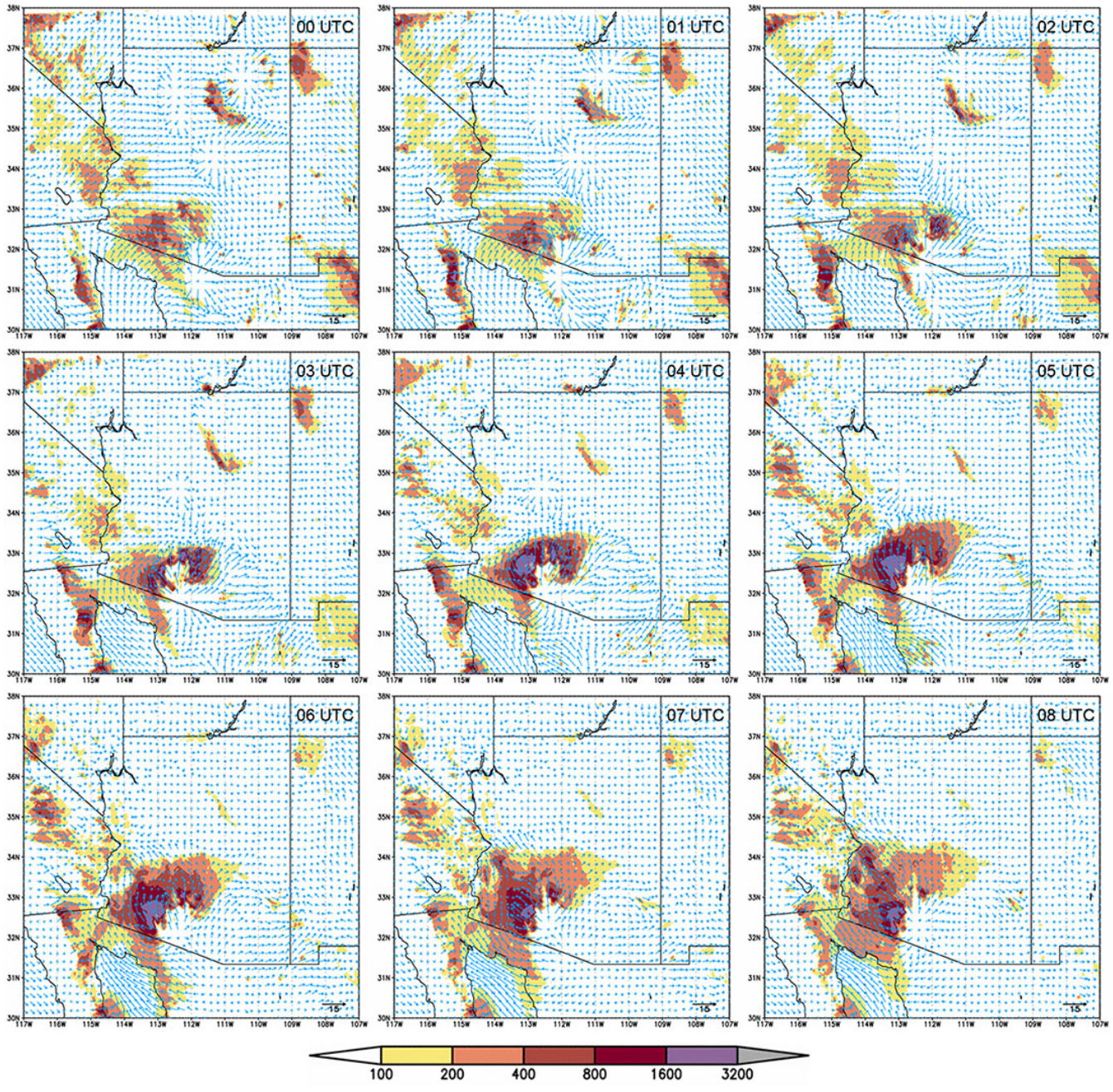

Fig. 2. NMME–DREAM PM_{10} surface dust concentration ($\mu g\,m^{-3}$) and wind on 10 m height ($m\,s^{-1}$), on every hour for the period 00:00–08:00 UTC 6 July 2011.

the WRF-Chem on 1.8 km resolution underestimated dust concentration, because their erodibility mask at 1° resolution is too coarse to describe sources properly over this region.

Simulation of the dust storm on 5 July 2011 on high resolution using the approach from the ENPHASYS project showed that real dust sources had not all been taken into account (Vukovic et al., 2011). Land cover types that could be dust productive are presented in Fig. 1, on the left panel. Open shrubland covers most of the region and it was necessary to correct the mask with introduction of these areas. According to Tegen at al. (2002), if NDVI is less or equal to 0.1 it can be considered as barren, and that open shrubland is 30–70 % covered with vegetation. We assumed that points classified as open shrubland with NDVI 0.1 or less are 100 % dust source. Areas with NDVI values increasing from 0.11 to 0.13 decreased linearly from 70 to 30 % as a dust source. The MODIS NDVI values assigned to 4 July 2011 are presented in Fig. 1, middle panel. The final mask in

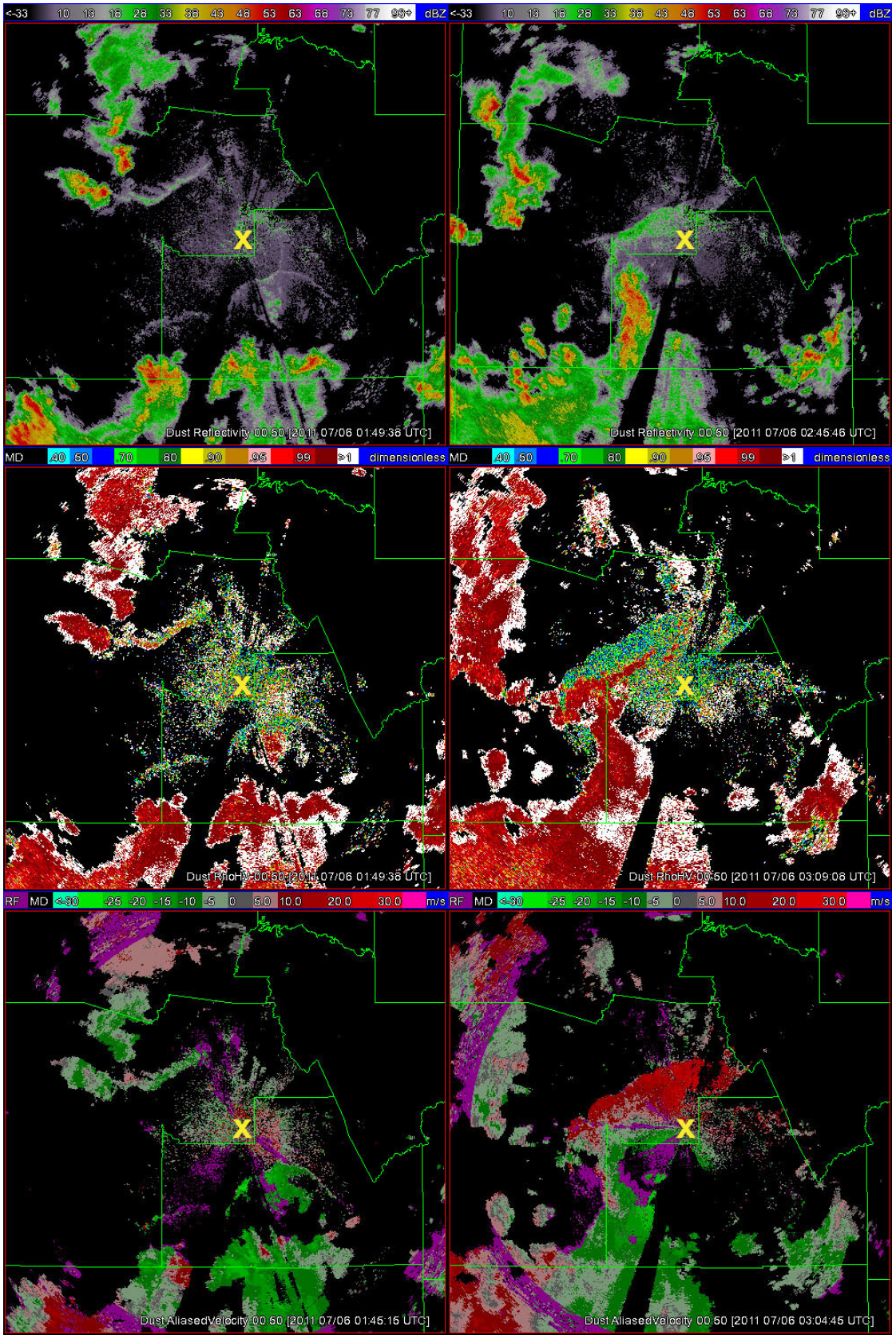

Fig. 3. Radar Z_{hh} at 01:50 (upper left) and 02:46 (upper right) UTC, ρ_{hv} at 01:50 (middle left) and 03:09 (middle right), and velocity at 01:45 (lower left) and 03:05 (lower right) UTC; radar location is marked with "x".

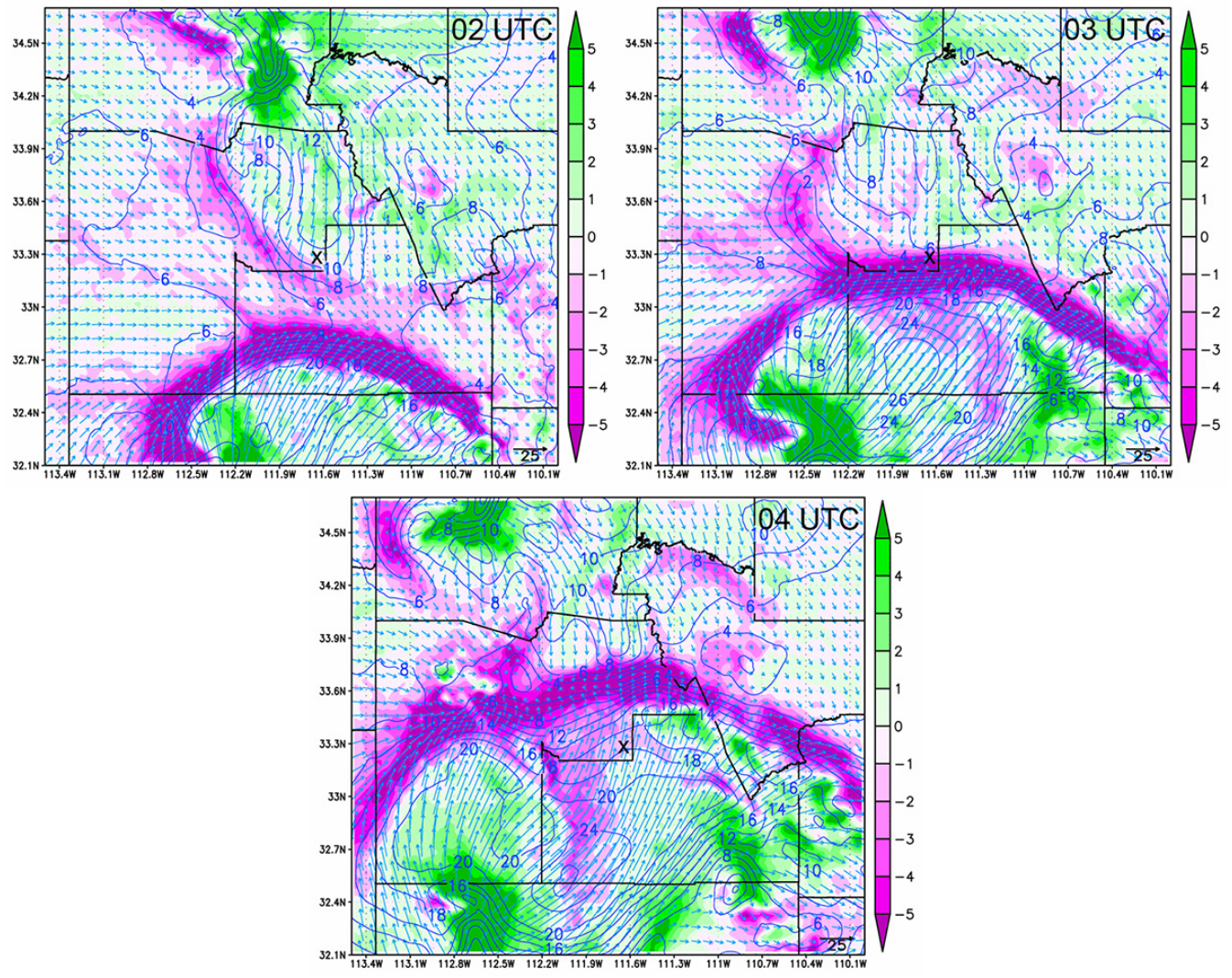

Fig. 4. NMME–DREAM wind at 11th model level (∼500m), divergence in $10^{-4}\,s^{-1}$ (green to purple), magnitude in m/s (blue lines), and direction (arrows) at 02:00 (upper left), 03:00 (upper right), and 04:00 (lower) UTC, respectively, 6 July 2011; radar location is marked with "x".

the model simulation combined the barren land cover type as 100 % dust productive, cropland as dust productive if NDVI was less then 0.25, and open shrub land as explained above. The mask specification, obtained using MODIS data with 500 m resolution, is considered as the mask of potential dust sources, since the dust uptake further depends on the soil texture, soil moisture and near-surface atmospheric conditions. This version of the mask is used in the NMME–DREAM for the numerical simulation of the 5 July 2011 dust storm, and it is presented in Fig. 1 (right panel) after being up-scaled (area averaged) into the model resolution. Information about the soil texture used by the model is from STATSGO-FAO soil map (US Department of Agriculture, 1994), available in 30 s resolution for USDA 12 soil texture classes. Following Shirazi (2001) and Tegen et al. (2002), clay and silt content is determined in each soil texture class in order to evaluate the amount of each particle mode in the model bins for the dust emission (Pérez et al., 2006).

4 Model results and discussion

Further analysis of model results focused on model validation using collected proxy information (e.g. citizen photos and first-hand accounts), measurements and observations related to the storm. Mechanisms that lead to the formation of the storm and its development were not studied. Comparison of model meteorology with observations is done to exclude effects of the quality of the atmospheric forecast when analyzing the dust forecast; this was done in order to distinguish conclusions about the dust model's ability to transport dust

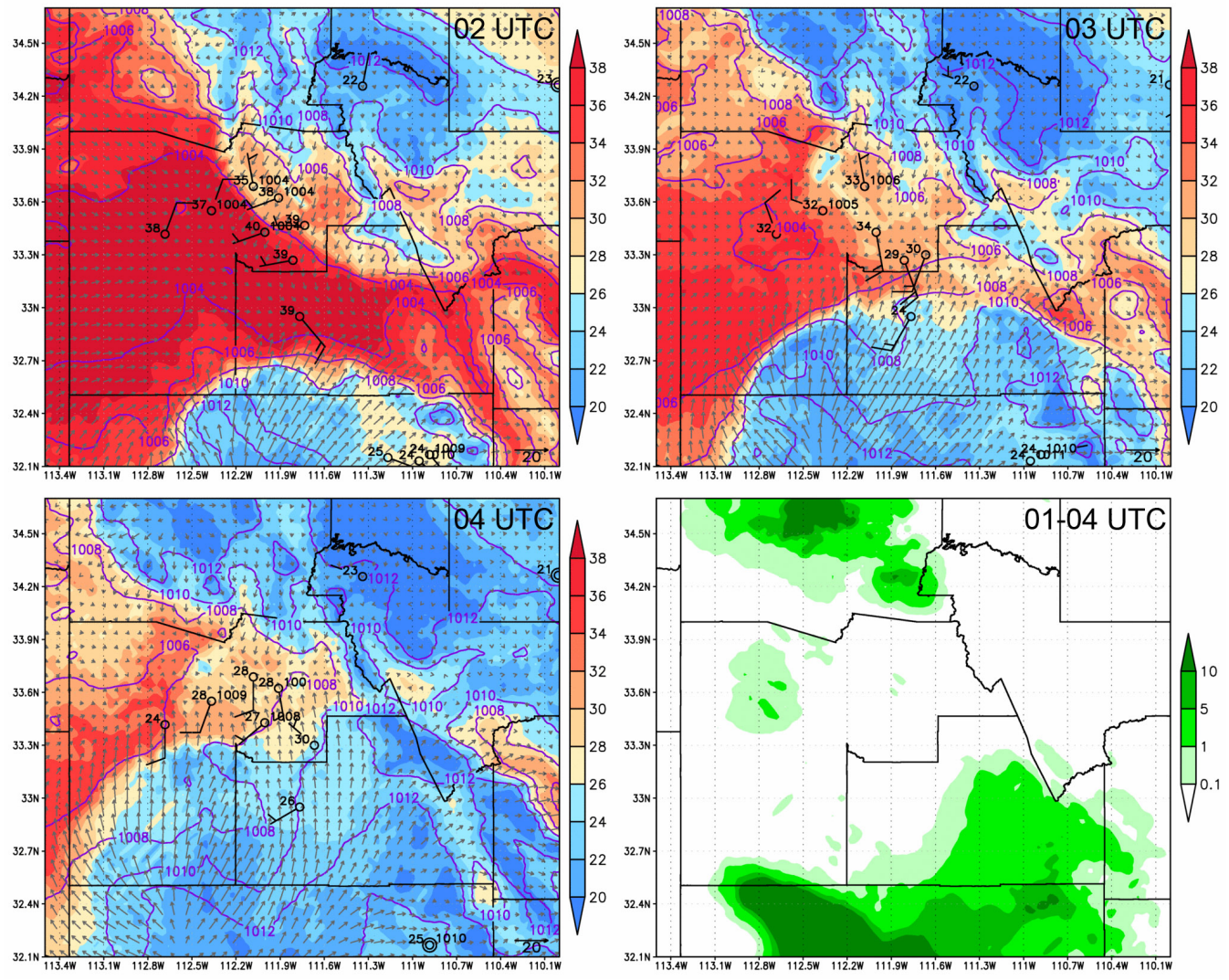

Fig. 5. NMME–DREAM 2 m temperature (blue to red), surface pressure (purple lines) and 10 m wind (arrows), and observed values at stations (2 m temperature, surface pressure and 10m wind) at at 02:00 (upper left), 03:00 (upper right), and 04:00 (lower left) UTC 6 July 2011; NMME–DREAM 3 h accumulated precipitation for the period 01:00–04:00 UTC, respectively, 6 July 2011 (lower right).

in such events. The main focus was to validate the timing and position of the haboob front movement toward Phoenix, and then to evaluate dust concentration transported within the dust model. Calculation of the statistical scores of the model performance will not be done since not enough observational data are available in the region captured in the entire event. Another problem encountered in dust verification is the great variability of dust in time and space on small scales. Point-on-point verification can lead to the so-called "double penalty problem" (Rossa et al., 2008).

Haboob dust storms are characterized in the model with the dust transport within the first 1–2 km of the lower atmosphere, implying the importance of the model surface dust concentration to describe the process. In Fig. 2 we present the NMME–DREAM PM_{10} surface dust concentration and 10 m wind for the selected period of model simulation (i.e. 00:00–08:00 UTC 6 July 2011, over the entire model domain). The strong downdraft outburst near the southern border of Arizona, first visible at 00:00 UTC, produced strong surface wind that propagates north and west, lifting dust along the way. The downburst of cold air generated an almost radial diverging pattern in the 10 m horizontal wind. During the time period 02:00–05:00 UTC, the event reached and passed over Phoenix. On its way north-northeast, the wind lost its strength and, by the end of the model simulation, dust concentrations decreased over the Phoenix area. To discuss the dust model performance further, we must first evaluate the atmospheric model forecast.

Routine meteorological observations available for this event were widely scattered over the model domain and are

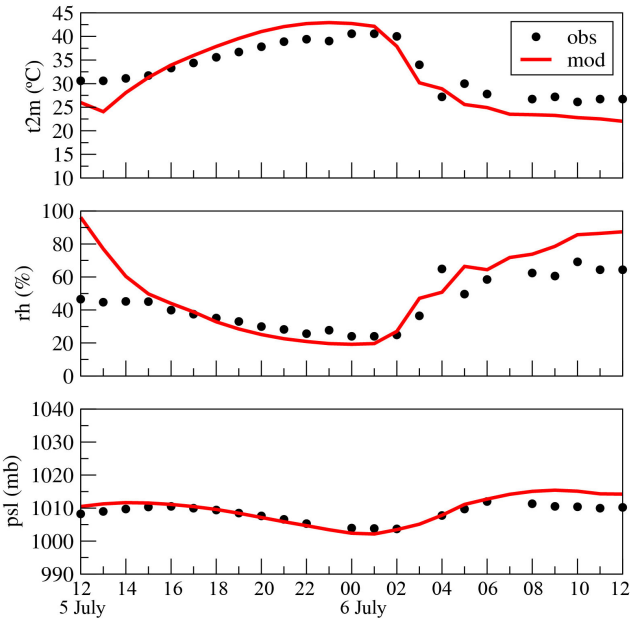

Fig. 6. NMME–DREAM and observed values at Phoenix/Sky Harbor station, 2 m temperature (upper), relative humidity (middle), and surface pressure (lower).

insufficient to obtain shape, path and timing of the storm since they do not cover most of the area of interest. To evaluate the atmospheric model performance we use images obtained from the KIWA Phoenix radar. The focus of further discussion will be on the selected region inside the model domain that is captured by the radar (32.1° N–34.7° N, 110° W–113.5° W). KIWA operated in volume coverage pattern 11 (VCP 11), which includes 14 constant-elevation angle sweeps from 0.58 to 19.58 degrees. The KIWA radar completes a scan in 5 min, and the range gate resolution is 1 km for reflectivity. Figure 3 presents several variables obtained from the radar, where the border of the dust storm, direction of movement and velocity are visible. The radar reflectivity factor, Z_{hh}, (Fig. 3, upper panels) shows the incoming front from the south-southeast, moving north-northwest. At 01:50 UTC, the storm front is south of Phoenix and approximately 30 km distant from the radar. At 02:45 UTC the front line is inside Phoenix, already past the radar location. Reflectivity strongly depends on particle size and concentration. Employing Z_{hh} alone (as is done with single-polarization radars) limits microphysical interpretation because of the inherent ambiguity associated with its measurement. For instance, two radar-sampling volumes, one containing large concentration of small particles and the other a smaller concentration of large particles, can yield similar Z_{hh} values. However, polarization diversity allows this distinction to be made. This study considers co-polar correlation coefficient, ρ_{hv}, as one of polarimetric variables, observed in the Phoenix dust storm. It is not known yet whether this is a signature of all dust storms or just of the intense ones, as this is the first dust storm to be sampled by a radar with dual polarization capabilities. The co-polar correlation coefficient is a measure of the correlation between the backscattered horizontal and vertical polarized signals from each scatterer within a sampling volume. It depends on particle orientations and shapes, as well as phase compositions within the radar sampling volume. For spherical particles of any size $\rho_{hv} \equiv 1$. In pure rain at S band, ρ_{hv} does not differ significantly from unity. Observations of slight decreases in ρ_{hv} in pure rain (no lower than ∼0.98 at S band) are attributed to randomness in orientations and oblateness diversity of raindrops. Furthermore, ρ_{hv} can decrease significantly for irregular scatterers such as hailstones with large protuberances (Balakrishnan and Zrnic, 1990), chaff (Zrnic and Ryzhkov, 2004), and debris (Ryzhkov et al., 2005); ρ_{hv} values below 0.8 indicate non-meteorological targets. Figure 3, middle panels, shows the correlation coefficient of about 0.5, which confirms the presence of dust, since only non-meteorological particles can cause such low values of ρ_{hv}. The front line that approaches from the south-southeast is moving approximately toward the radar, so the Doppler radar velocity can be considered as valid (Fig. 3, lower panels). While approaching, velocity is negative. After the storm passes the radar point velocities are positive. Radar data are used to verify position of the front, direction of the movement and velocity.

The simulated wind at the height of about 500 m is chosen to compare with the radar images because it is the approximate height the radar depicts at the selected times and locations of the front. Figure 4 displays the divergence, the magnitude and direction of the wind at 02:00, 03:00 and 04:00 UTC 6 July 2011. The divergence field marks the front position. Where it is negative, there is convergence and strong upward movement. Comparing the radar (Fig. 3) and the model (Fig. 4) images, we can confirm that position and the direction of the front line is approximately good, but the model is about 1 h late. Model wind velocity is over 20 m/s, which is also visible in the radar data. The model front may be late because of blocking by the approaching cold air from the north that met the front line earlier than in reality. This would have slowed frontal movement. It may also be that the center of the haboob is shifted west in the model, and the wind energy is not strong enough to push toward the north, as it actually happened. The cause cannot be explained with certainty because of the lack of observations. Despite these differences, the model results about the front line position, direction of the movement and the velocity are considered very similar to the radar data. The atmospheric component of NMME–DREAM produced a downburst and wind energy strong enough to generate the haboob.

Performance of the atmospheric model near the surface is presented in Fig. 5. Available observations of the temperature at 2 m, surface pressure, and 10 m wind are presented on the same image at meteorological station locations. The front line is clearly visible from the model temperature field and is

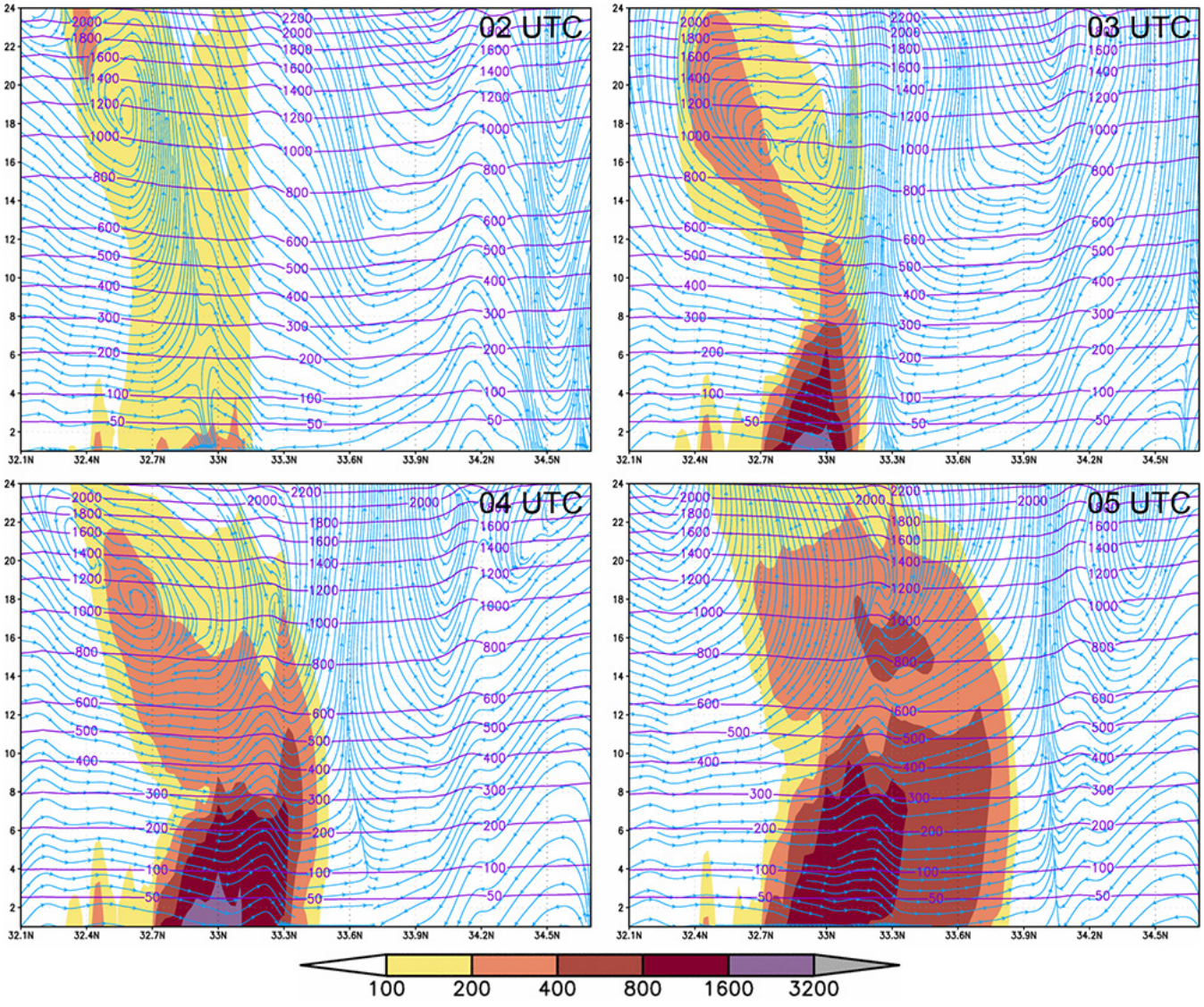

Fig. 7. NMME–DREAM vertical cross section along 112.2 ° W, PM_{10} dust concentration, streamlines (blue), and height of model levels (purple lines) at 02:00 (upper left), 03:00 (upper right), 04:00 (lower left), and 05:00 (lower right) UTC, respectively, 6 July 2011.

in good agreement with observed values. A rise in the surface pressure follows a decrease in temperature. Observed surface wind is obtained as the average value of the 10 min data. The model value is shown exactly at full hour marks. Because of large surface wind variability, and the fact that this was the time with wind gusts that are not likely to coincide in time with model calculations, it is more difficult to obtain a credible conclusion about the wind field using anemometer data than when validating against radar data. The 1 h later arrival of the front line is also visible in the surface wind. The model did generate precipitation in the downburst areas (Fig. 5), but no ground measurements were available for comparison. On the dust storm path toward Phoenix, over the most active of dust sources that day, both model and observations showed no precipitation. This indicates that wet deposition parameterization is not the cause for dust loss in the model when entering Phoenix. We cannot comment further on modeled precipitation and its impact on the dust forecast due to lack of observational data. Figure 6 presents Phoenix/Sky Harbor observed values for the 2 m temperature, relative humidity (calculated from the 2 m temperature and dew point) and surface pressure against the model data. This specific station is selected since data were available on every hour during the event. Other meteorological stations mostly had interruptions in the measurements. It is obvious that temperature in the model initial field at this location is 5 °C colder than observed values, which led to the large difference in the values of relative humidity. Despite this difference at the initial moment of the model simulation, the model corrected these values after several hours. Change in surface variables, large decrease

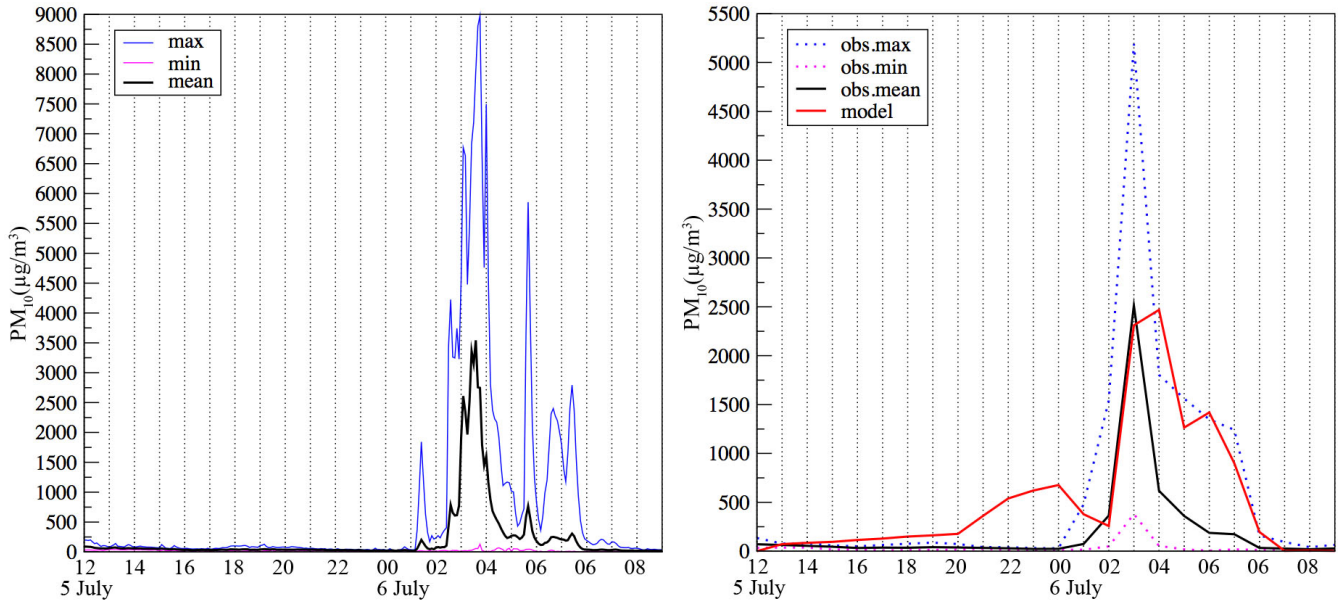

Fig. 8. Observed values of PM_{10} on 5 min in all 11 stations in Maricopa (left), and values at full hour with model PM_{10} surface dust concentration at selected point.

in temperature (over 10 °C during one hour), increase in the humidity and change in the surface pressure are well represented by the model during the event. After the storm, temperature stopped decreasing, but the model-simulated temperatures were lower than observed. This may be the influence of concrete urban areas that accumulated heat during the day, or it may be due to the difference between model and reality in the position of the cold air from the north when it meets the frontal line.

Atmospheric model evaluation showed that weather conditions that drive the dust storm are simulated very well. We can assume that meteorology in the coupled atmospheric-dust model is correct, but should expect about 1 h later arrival of the dust in the Phoenix. This means that, in further discussion about model performance, and accounting for later dust arrival in the model, we can exclude atmospheric model quality and analyze the data as the product of the dust model alone.

Vertical distribution of the dust, simulated by the model, is presented in Fig. 7. Selected cross section is along 112.2° W, where high dust concentration at near-surface levels, vertical mixing, and the front line with upward movement are noticeable. This cross section is selected because it represents the dust front movement toward central Phoenix. During the period 02:00–05:00 UTC formation of the dust storm and its movement toward Phoenix is visible. Height of the dust storm approximately coincides to the height evaluated by the NWS Forecast Office. Solenoidal circulation, a horizontal vortex within cool air in the frontal area (behind the front line), is characteristic for the haboob and is visible from the streamlines with the center of rotation at about 1 km height.

Figure 8, left panel, depicts variability of PM_{10}, and the real intensity of the dust storm. Presented here are measured values of PM_{10} every 5 min, maximum, minimum and mean value obtained from the 11 sites in Maricopa County, but mainly located in the Phoenix metropolitan area. Highest concentrations are measured in the period 03:00–04:00 UTC, with a maximum reaching 9000 µg m^{-3}. Variability in the concentrations between stations is almost two orders of magnitude. Concentration change in time is also very rapid and intense, about several 1000 µg m^{-3}. Model results available at every full hour are compared with observed values at the same times (Fig. 8, right panel). Peak in model concentration at the same time as the observed values is south of the region with observations. This is likely due to the previously discussed later arrival of the front. An example of the model PM_{10} surface dust concentration at 33° N, 112.2° W is presented by the red line. The selected model point is located south of the observations because the model front at the time of the highest measured concentrations arrived at this location, and we know about the 1 h delay of the atmospheric forecast. Thus, the true potential of the dust model performance is seen more clearly than if the point in the city where the measurements are located is chosen. Furthermore, the model loses dust when the front enters the city. Model concentrations in the area with observations are 300–700 µg m^{-3}, which is shown in Figs. 9 and 10. The rapid increase in model values of concentration, magnitude and duration of the event agrees with observed values. Highest concentrations are noted during the period 03:00–05:00 UTC, for which the model PM_{10} surface dust concentration and observed values at stations in Fig. 9 are shown. Solomos

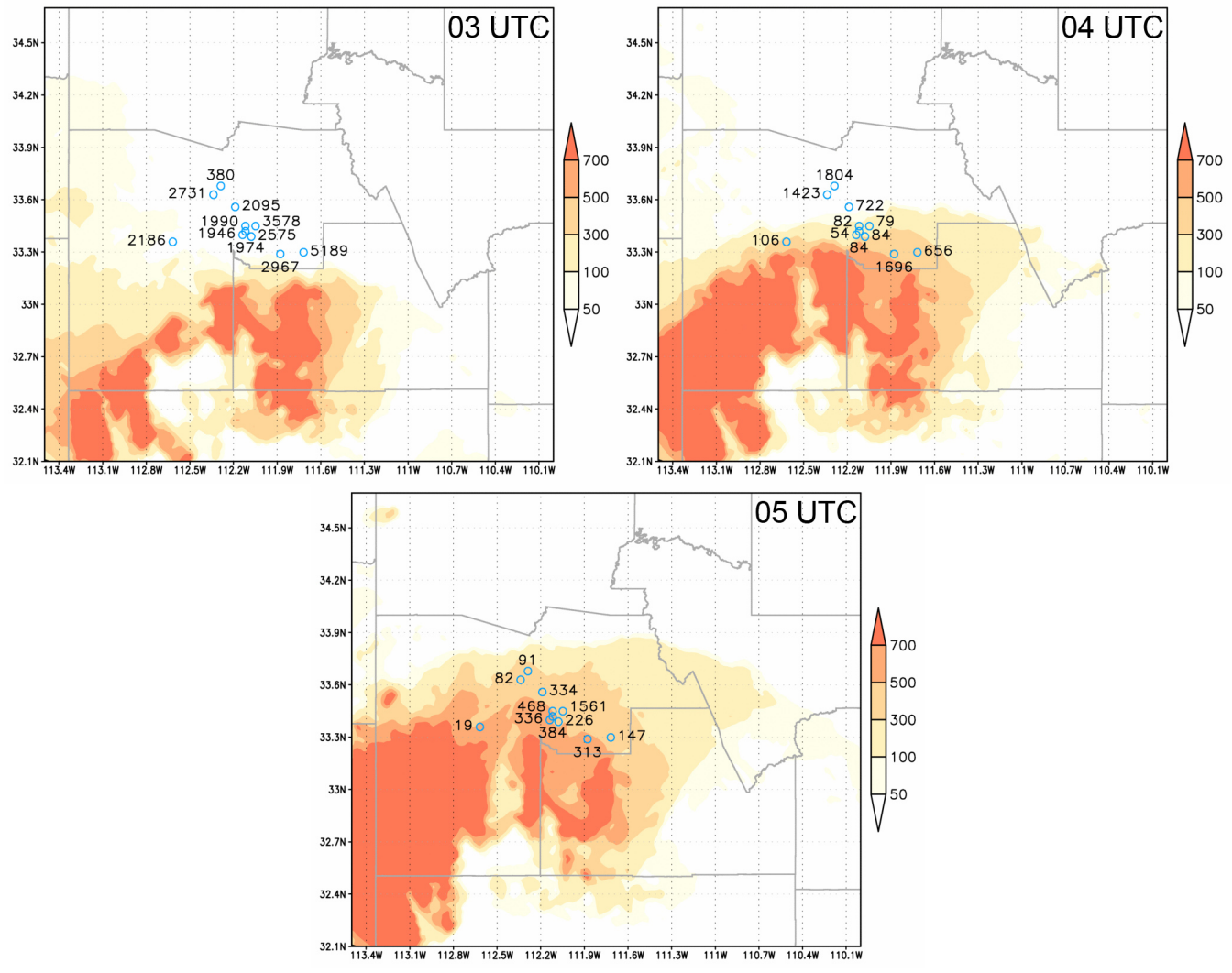

Fig. 9. NMME–DREAM PM_{10} surface dust concentration and observed values of PM_{10} ($\mu g\,m^{-3}$) at 03:00 (upper left), 04:00 (upper right), and 05:00 (lower) UTC 6 July 2011.

et al. (2012) summarized the flow structure during the dust episode driven by density currents. Dust productivity is increased behind the front line, due to increased turbulence near the surface. Meteorological and PM_{10} observations, and numerical model simulation results in this case also show the characteristics of the flow structure explained by the authors. The dust storm in the model simulation did not reach Phoenix at 03:00 UTC, although its presence is clearly visible in the observations. During the next 2 hours the simulated dust storm crossed over Phoenix, but lost its intensity entering the Phoenix area. In general, the dust model managed to simulate the shape, height and movement of the dust storm that is in agreement with the collected knowledge on the event, with some underestimation of PM_{10} concentration.

The modeled dust concentration in the Phoenix area is $\sim$500 $\mu g\,m^{-3}$, several times less than observed. Since the atmospheric model performed well, the low concentration is likely attributed to the dust model. Actual attribution is problematic. The main cause of such differences between the model and measurements might be related to parameterization of the dust sources and processes related to dust. So far, dust models are mainly tested over large desert regions with rather homogeneous distribution of dust sources, using much coarser resolutions. Such models are adjusted to properly simulate events of larger scales. This raises the question if the same dust-related parameterization can be used on regional and local scales, for example, use of different emission schemes (Sundram et al., 2004) or different convective dust mixing schemes (Pérez et al., 2011). Another source of uncertainty: the observations themselves. PM_{10} observations include particles of different origin that are not simulated in this setup of DREAM.

Another uncertainty is the definition of the mask of potentially dust productive areas. To demonstrate the sensitivity

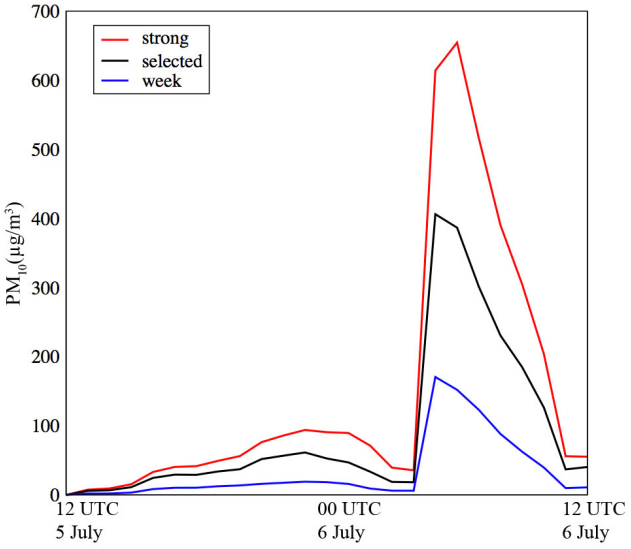

Fig. 10. NMME–DREAM PM_{10} surface dust concentration in Phoenix for different masks of potential dust sources.

of the dust model on the definition of the dust mask, model PM_{10} surface dust concentration is shown in Fig. 10 for the point located in Phoenix (33.4° N, 112.1° W), which is obtained with three different masks. The meteorology is the same in all three cases, so the timing of peaks is the same, but intensity is different. The blue line (weak) is obtained from the model simulation with the mask that includes only barren and cropland land cover types. The black line (selected) is from the model simulation discussed in this paper: open shrubland area with NDVI up to 0.13 is added in the mask. The red line (strong) is obtained from the model simulation with the mask that includes open shrubland area with NDVI up to 0.15. PM_{10} increased over 200 $\mu g\,m^{-3}$ when open shrubland was included and approximately the same amount with the strong mask. The model dust concentration in Phoenix can be increased to the level of the observed values in this way, but this can cause dust uptake over too large an area of the model domain. Dust concentration observations are needed from the source regions south of Phoenix (Pinal county), where much of this dust originates, in order to see if this is the right solution. Better calibration of the mask was not possible in this case. In the simulations, the mask selected had reproduced the shape of the dust storm. Overall, it compared well with the observational knowledge on the event. Unfortunately, the sum of observational dust evidence made good model verification and validation impossible; model verification became more descriptive than quantitative.

5 Model validation using satellite observations

Based on the previous analysis, it is quite clear that the haboob event is well detected and its dynamical and physical features are examined in detail using dynamic numerical modeling. Our research has benefitted from earth-viewing satellite sensors and an integrative approach to dust storm simulations and forecasts. Here we present satellite evidence for the occurrence and development of the event under investigation. Satellite remote sensing is expedient in monitoring various aspects of dust storms in both space and time (e.g. King et al., 1999; El-Askary et al., 2003, 2004, 2006; Shao and Dong, 2006; Li et al., 2007; Xu et al., 2011). During this haboob, synergistic methods are applied to detect and monitor the event for model validation using multi-temporal and/or multi-sensor approaches. These approaches have been applied to detect and monitor sand and dust storms in various regions including the Nile Delta (El-Askary et al., 2003, 2009; Prasad et al., 2010; Marey et al., 2010, 2011) and the Indo–Gangetic basin (El-Askary et al., 2006; Prasad et al., 2006; Prasad and Singh, 2007). In this work we used the aerosol optical depth (AOD), which is a measure of the opaqueness of air, using the retrieval algorithm known as deep blue (DB). It is applied over bright surfaces such as deserts and other arid land surfaces by incorporating two blue channels (0.412 and 0.470 µm), with uncertainties reported to be around 25–30 % (Hsu et al., 2004, 2006). High values indicate poor visibility. Ginoux et al. (2010) were able to identify anthropogenic and natural dust sources using the MODIS DB algorithm along with land use data.

We also used CALIPSO, which is a Franco–American mission that supplies a unique data set of atmospheric vertical profiles measured by CALIOP onboard the satellite with a 30 m vertical resolution to measure aerosol and cloud properties (Winker et al., 2004). The profiles range from the surface to 40 km with a resolution of 30–60 m in the vertical and 333 m in the horizontal. CALIPSO can detect optical depths of 0.01 or less, so it can observe weak aerosol layers and thin clouds (McGill et al., 2007).

In this study, the CALIOP Level 1B data were employed, which contain calibrated and geolocated single-shot (highest resolution) lidar profiles. Nighttime CALIOP profiles are generally better as they depict dust storms more accurately compared to daytime overpass data that are noisier (Labonne et al., 2007). In Fig. 11, the vertical profiles of the atmosphere up to 30 km, represented by total attenuated backscatter at 532 nm, are shown as CALIPSO passes over Arizona and our region of interest on 6 July (Fig. 11a, c) during night and day, respectively. Figure 11b and d showed the most abundant aerosol types over selected areas shown in Fig. 11a, b. Each profile clearly shows the vertical structure of a major haboob over the study regions in agreement with model results. All the abundant aerosol types ranged from dust to polluted dust and smoke, all of which contribute in the development of the

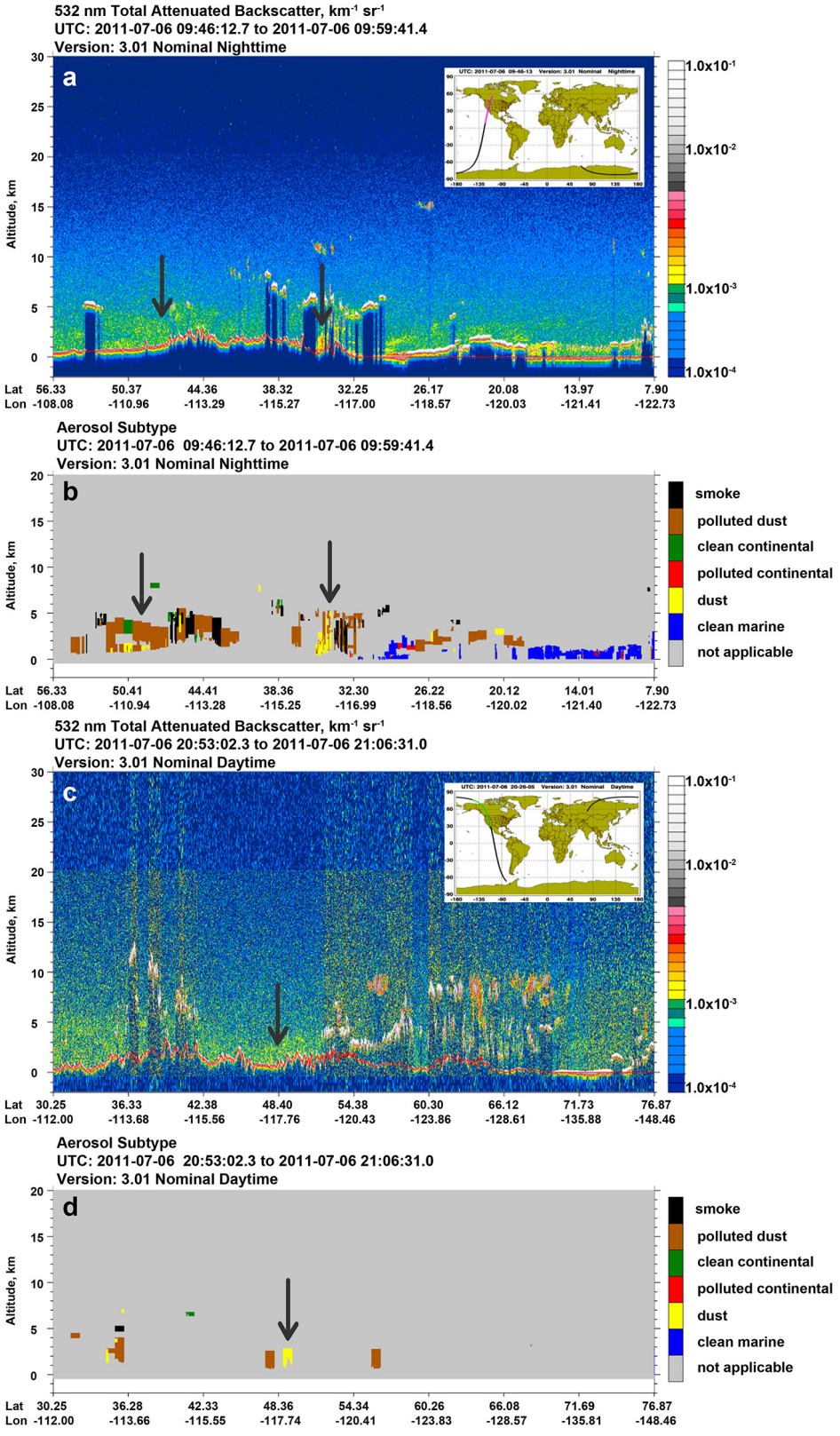

Fig. 11. Satellite observations of haboob event 6 July 2011 showing total attenuated backscatter at 532 nm of a dust event as measured by **(a)** the nighttime CALIPSO overpass (at 09:46 to 09:59 UTC) and **(c)** the daytime CALIPSO overpass (at 20:53 to 21:06 UTC) and CALPSO aerosol subtype at **(b)** nighttime and **(d)** daytime. The inset map shows the path of CALIPSO overpass over the globe (black line) and the study region (magenta "night" and green "day" lines).

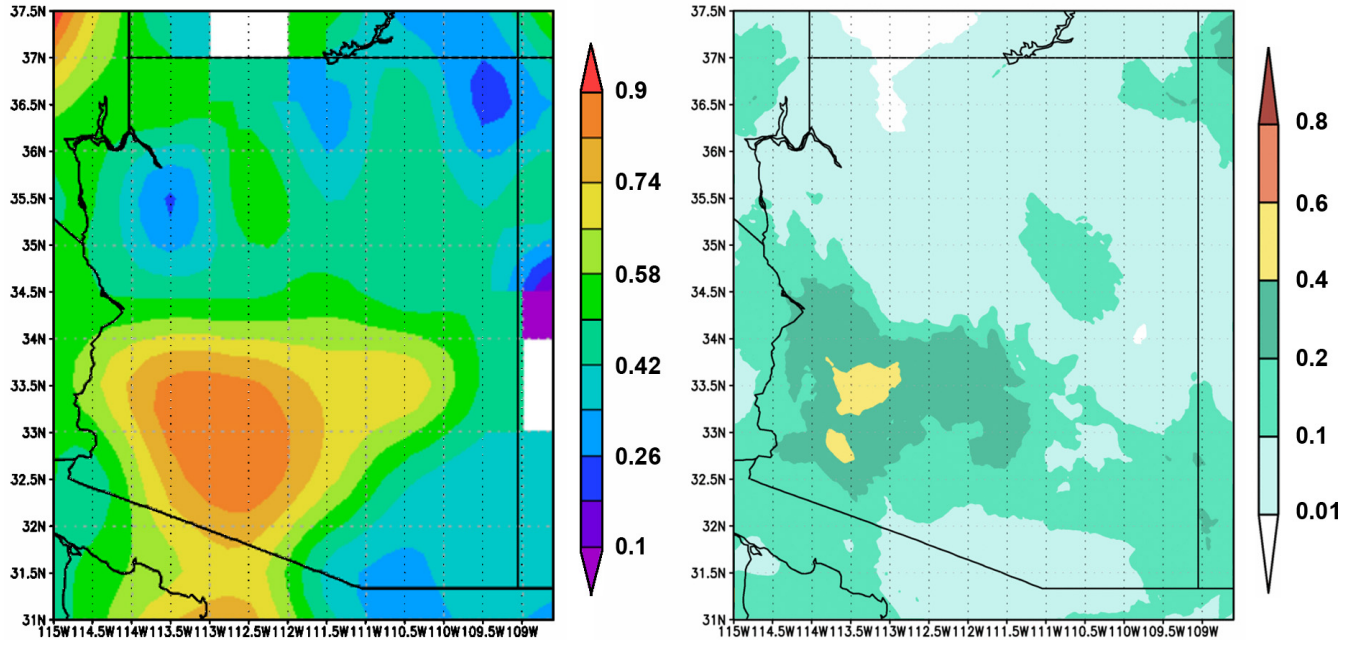

Fig. 12. Aqua MODIS aerosol optical depth (AOD) based on deep blue (DB) algorithm (left) and NMME–DREAM AOD (right) for the nighttime overpass time.

haboob and suggest further that non-desert dust sources may have contributed to the higher levels of observed PM_{10}.

Figure 12 shows Aqua MODIS aerosol optical depth (AOD) based on DB algorithm and NMME–DREAM AOD for the nighttime overpass time. Observed AOD shows high agreement with the PM_{10} model simulation (Fig. 2) and with model AOD pattern. Comparison of model and satellite data show that the model performed well over the domain but, once again, proper quantitative validation was not possible considering the lack of observations and the uncertainty of satellite AOD.

6 Conclusions

About 40 years after the American haboob was recognized over the southwest US, computer power, modeling of atmospheric processes, and satellite observations advanced to the point where we are able to simulate such an extreme and local dust storm event. Dust numerical models are developed to simulate dust transport on global or regional level. Behavior of high-resolution dust models that simulate intense dust events of relatively small spatial and temporal scales, like the dust storm on 5 July 2011, is not well known. Parameterizations of the processes related to the dust cycle are generally tested and adjusted to work on much coarser resolutions and for simulation of long-range dust transport. Because of the characteristic intense convective movements of an haboob, it is necessary to use a non-hydrostatic atmospheric model. High-resolution model runs are also necessary because of the nature of the potentially dust productive areas in the southwest US. To simulate the American haboob, we used a regional coupled atmospheric-dust model NMME–DREAM. The model resolution was 4 km. Despite the fact that DREAM model never has been applied in the simulation of such events, it managed to produce an accurate shape, duration and magnitude of the dust storm. No changes were made in the parameterization of the physical processes related to dust. Definition of the dust source mask is a principal cause for the success of the presented results. Distribution of potentially dust productive areas depends on season of the year, agricultural cycles, land use practices and differs from year to year depending on precipitation during the previous months. The mask used in this case is obtained from latest NASA MODIS land cover and NDVI data. Verification of results showed that the atmospheric part of the model performed very well, with the front arrival at Phoenix being one hour late. Analysis of the dust model showed that the model produced a peak in dust concentration of $\sim 2500\,\mu g\,m^{-3}$, over the closest source regions south of Phoenix. Over Phoenix, the model underestimated concentration values compared to PM_{10} measurements. The reason for this discrepancy is unclear: is it model parameterization of the dust cycle or is it the definition of the mask of potentially dust productive areas? Further analysis and possible improvements of the dust model and the sources require more measurements not yet available to the community. Better understanding of the model performance and improvement, and general conclusion on model quality require a longer period of simulation that includes various dust events

as well as periods with no dust being transported. Longer period simulation will enable model quantitative verification (i.e. calculation of model scores). This will be the focus of the future work. When high-resolution specification of regularly updated dust sources are used in other non-hydrostatic models that include dust transport, these other models can significantly improve their performance over regions with small-scale, point-like dust sources that change in time, as is the case in the southwest US. Dust model inter-comparisons can improve our knowledge and accelerate progress in high-resolution dust modeling. This will lead to reliable, credible dust forecast systems of the future.

Results encourage further development and use of dust models as tools for warning and for risk mitigation policy. Windblown dust and particularly haboobs can have disastrous consequences for traffic and health. Besides improving model PM_{10} results, dust models should be enabled to simulate the transport of even larger dust particles, which is often ignored because they tend to settle down quickly and do not travel great distances. But, over the southwest US where dust sources can be very close to populated areas and major airway and highway traffic, they significantly affect air quality and visibility.

Acknowledgements. The authors recognize Mr. Raymond Gaddi, a senior intern from Troy High School in Orange, California, for his assessment of climatic conditions leading up to the 5 July 2011 haboob. The work reported herein was supported by several sources: by the project "Development and Implementation of a Climate Change Module for Environmental Public Health Tracking Utilizing Remote Sensing Data and Airborne Dust Models: a Tool in Environmental health Tracking", by the US Centers for Disease Control and Prevention and the National Aeronautics and Space Administration's program in Applied Sciences for Health and Air Quality under contract NNM08AA04A; by the South East European Virtual Climate Change Center (hosted by the Republic Hydrometeorological Service of Serbia). The work presented in this paper is also part of the project "Studying climate change and its influence on the environment: impacts, adaptation and mitigation" (43007) financed by the Ministry of Education, Science and Technological Development of the Republic of Serbia. Authors gratefully acknowledge this support.

Edited by: G. Kallos

References

Adams, D. K. and Comrie, A. C.: The North American Monsoon. Bull. Amer. Meteor. Soc., 78, 2197–2213, 1997.

Balakrishnan, N. and Zrnic, D. S.: Use of polarization to Characterize precipitation and discriminate large hail. J. Atmos. Sci., 47, 1525–1540, 1990.

Balis, D., Amiridis, V., Kazadzis, S., Papayannis, A., Tsaknakis, G., Tzortzakis, S., Kalivitis, N., Vrekoussis, M., Kanakidou, M., Mihalopoulos, N., Chourdakis, G., Nickovic, S., Pérez, C., Baldasano, J., and Drakakis, M.: Optical characteristics of desert dust over the East Mediterranean during summer: a case study, Ann. Geophys., 24, 807–821, doi:10.5194/angeo-24-807-2006, 2006.

Chamberlain, A. C.: Roughnessle ngth of sea, sand and snow, Bound. Layer Meteorol., 25, 405–409, 1983.

Chen, W. and Fryrear, D.: Sedimentary characteristics of a haboob dust storm, Atmos. Res., 61, 75–85, 2002.

Claquin, T., Schulz, M., and Balkanski, Y.: Modeling the mineralogy of atmospheric dust sources, J. Geophys. Res., 104, 22243–22256, 1999.

Douglas, M. W., Maddox, R. A., Howard, K., and Reyes, S.: The Mexican monsoon. J. Climate, 6, 1665–1667, 1993.

El-Askary, H., Sarkar, S., and El-Ghazawi, T. A.: Multisensor approach to dust storm monitoring over the Nile delta, IEEE Trans. Geosci. Remote Sens., 41, 2386–2391, 2003.

El-Askary, H., Gautam, R., and Kafatos, M: Remote sensing of dust storms over the Indo-Gangetic basin, J. Indian Soc. Remote Sens., 32, 121–124, 2004.

El-Askary, H., Gautam, R., Singh, R. P., and Kafatos, M.: Dust storms detection over the Indo-Gangetic basin using multi sensor data, Adv. Space Res., 37, 728–733, 2006.

El-Askary, H., Farouk, R., Ichoku, C., and Kafatos, M.: Transport of dust and anthropogenic aerosols across Alexandria, Egypt, Ann. Geophys., 27, 2869–2879, doi:10.5194/angeo-27-2869-2009, 2009.

Emmel, C., Knippertz, P., and Schulz, O.: Climatology of convective density currents in the southern foothills of the Atlas Mountains, J. Geophys. Res., 115, D11115, doi:10.1029/2009JD012863, 2010.

Estes, S. M., Haynes, J. A., Sprigg, W. A., Morain, S. A., and Budge A.: Using NASA Satellite Remote Sensing To Identify Dust and Sand Storms That Aggravate Respiratory Diseases, doi:10.1164/ajrccm-conference.2009.179.1_MeetingAbstracts.A3662, 2009.

Foster, R. J.: General Geology, Charles E. Merrill Publishing Company, Columbus, OH, 721 pp., 1969.

Freeman, L. H.: Duststorms of the Anglo-Egyptian Sudan, Meteor. Reports 2, 11, Great Britain Met. Office Publication, 22 pp., 1952.

Fujita, T. T.: The Downburst, Microburst and Macroburst, Report of Projects NIMROD and JAWS, Chicago, 122 pp., 1986.

Gillette, D. A., Clayton, R. N., Mayeda, T. K., Jackson, M. L., and Sridhar, K.: Tropospheric aerosols from some major dust storms of the southwestern United States, J. Appl. Meteorol., 17, 832–845, 1978.

Gillette, D. A., Adams, J., Endo, A., Smith, D., and Kihl, R.: Threshold Velocities for Input of Soil Particles Into the Air by Desert Soils, J. Geophys. Res., 85, 5621–5630, doi:10.1029/JC085iC10p05621, 1980.

Ginoux, P., Chin, M., Tegen, I., Prospero, J., Holben, B., Dubovik,O., and Lin, S. J.: Sources and distributions of dust aerosols simulated with the GOCART model, J. Geophys. Res., 106, 20255–20273, 2001.

Ginoux, P., Garbuzov, D., and Hsu, N. C.: Identification of anthropogenic and natural dust sources using Moderate Resolution Imaging Spectroradiometer (MODIS) Deep Blue level 2 data, J. Geophys. Res., 115, D05204, doi:10.1029/2009JD012398, 2010.

Hales Jr., J. E.: A severe southwestern desert thunderstorm: 19 August 1973, Mon. Weather Rev., 103, 344–351, 1975.

Haustein, K., Pérez, C., Baldasano, J. M., Mu¨ller, D., Tesche, M., Schladitz, A., Freudenthaler, V., Heese, B., Esselborn, M., Weinzierl, B., Kandler, K., and Hoyningen-Huene, W. Von: Regional dust model performance during SAMUM 2006, Geophys. Res. Lett., 36, L03812, doi:10.1029/2008GL036463, 2009.

Hsu, N. C., Tsay, S. C., King, M. D., and Herman, J. R.: Aerosol properties over bright-reflecting source regions, IEEE Trans. Geosci. Remote Sens., 42, 557–569, 2004.

Hsu, N. C., Tsay, S. C., King, M. D., and Herman, J. R.: Deep blue retrievals of Asian aerosol properties during ACE-Asia, IEEE Trans. Geosci. Remote Sens., 44, 3180–3195, 2006.

Hu, Q. and Feng, S.: Interannual Rainfall Variations in the North American Summer Monsoon Region: 1900–98*, J. Climate, 15, 1189–1202, 2002.

Idso, S. B.: Haboobs in Arizona. Weather 28, 154–155, 1973.

Idso, S. B.: Dust Storms, Sci. Am., 235, 108–114, 1976.

Idso, S. B., Ingram, R. S., and Pritchard, J. M.: An American Haboob, B. Am. Meteorol. Soc., 53, 930–955, 1972.

Janjic, Z. I.: The Step-Mountain Eta Coordinate Model: Further Developments of the Convection, Viscous Sublayer, and Turbulence Closure Schemes, Mon. Weather Rev., 122, 927–945, 1994.

Janjic, Z. I.: A nonhydrostatic model based on a new approach. Meteor. Atmos. Phys., 82, 271–285, 2003.

Janjic, Z. I., Gerrity Jr., J. P., and Nickovic, S.: An Alternative Approach to Nonhydrostatic Modeling, Mon. Weather Rev., 129, 1164–1178, 2001.

Jimeìnez-Guerrero, P., Peìrez, C., Jorba, O., and Baldasano, J. M.: Contribution of Saharan dust in an integrated air quality system and its on-line assessment, Geophys. Res. Lett., 35, L03814, doi:10.1029/2007GL031580, 2008.

Johnson, B. T., Brooks, M. E., Walters, D., Woodward, S., Christopher, S., and Schepanski, K.: Assessment of the Met Office dust forecast model using observations from the GERBILS campaign, Q. J. Roy. Meteorol. Soc., 137, 1131–1148, doi:10.1002/qj.736, 2011.

King, M. D., Kaufman, Y. J., Tanré, D., and Nakajima, T.: Remote sensing of tropospheric aerosols from space: Past, present, and future, B. Am. Meteor. Soc., 80, 2229–2259, 1999.

Knippertz, P. and Todd, M. C.: Mineral dust aerosols over the Sahara: meteorological controls on emission and transport and implications for modeling, Rev. Geophys., 50, RG1007, doi:10.1029/2011RG000362, 2012.

Knippertz, P., Deutscher, C., Kandler, K., Muller, T., Schulz, O., and Schutz L.: Dust mobilization due to density currents in the Atlas region. Observations from the Saharan Mineral Dust Experiment 2006 field campaign, J. Geophys. Res., 112, D21109, doi:10.1029/2007JD008774, 2007.

Knippertz, P., Trentmann, J., and Seifert, A.: High-resolution simulations of convective cool pools over the northwestern Sahara, J. Geophys. Res., 114, D08110, doi:10.1029/2008JD011271, 2009.

Labonne, M., Breon, F. M., and Chevallier, F.: Injection height of biomass burning aerosols as seen from a spaceborne lidar, Geophys Res Lett, 34, L11806, doi:10.1029/2007GL029311, 2007.

Lawson, T. J.: Haboob structure at Khartoum, Weather, 26, 105–112, 1971.

Lee, J. A., Gill, T. E., Mulligan, K. R., Dominguez Acosta, M., and Pérez, A. E.: Land Use/Land Cover and Point Sources of the 15 December 2003 Dust Storm in Southwestern North America, Geomorphology, 105, 18–27, doi:10.1016/j.geomorph.2007.12.016, 2009.

Li, J., Zhang, P., Schmit, T. J., Schmetz, J., and Menzel, W. P.: Quantitative monitoring of a Saharan dust event with SEVIRI on Meteosat-8, Int. J. Remote Sens., 28, 2181–2186, 2007.

Marey, H. S., Gille, J. C., El-Askary, H. M., Shalaby, E. A., and El-Raey, M. E.: Study of the formation of the “black cloud" and its dynamics over Cairo, Egypt, using MODIS and MISR sensors, J. Geophys. Res., 115, D21206, doi:10.1029/2010JD014384, 2010.

Marey, H. S., Gille, J. C., El-Askary, H. M., Shalaby, E. A., and El-Raey, M. E.: Aerosol climatology over Nile Delta based on MODIS, MISR and OMI satellite data, Atmos. Chem. Phys., 11, 10637–10648, doi:10.5194/acp-11-10637-2011, 2011.

Marsham, J. H., Knippertz, P., Dixon, N. S., Parker, D. J., and Lister, G. M. S.: The importance of the representation of deep convection for modeled dust-generating winds over West Africa during summer, Geophys. Res. Lett., 38, L16803, doi:10.1029/2011GL048368, 2011.

McGill, M. J., Vaughan, M. A., Trepte, C. R., Hart, W. D., Hlavka, D. L., Winker, D. M., and Kuehn, R.: Airborne validation of spatial properties measured by the CALIPSO lidar, J. Geophys. Res., 112, D20201, doi:10.1029/2007JD008768, 2007.

Morain, S. A., Sprigg, W. A., Benedict, K., Budge, A., Budge, T., Hudspeth, W., Barbaris, B., Yin, D., and Shaw, P.: Public Health Applications in Remote Sensing: Verification and Validation Report, NASA Coorperative agreement NNS04AA19A, 2007.

Morain, S. A., Sprigg, W. A., Benedict, K., Budge, A., Budge, T., Hudspeth, W., Sanchez, G., Barbaris, B., Catrall, C., Chandy, B., Mahler, A. B., Shaw, P., Thome, K, Nickovic, S., Yin, D., Holland, D., Spear, J., Simpson, G., and Zelicoff, A.: Public Health Applications in Remote Sensing: Final Benchmark Report, NASA Coorperative agreement NNS04AA19A, 2009.

Nickovic, S.: Dust Aerosol Modeling: Step Toward Integrated Environmental Forecasting, Eos. Trans. AGU, 83, Fall Meeting, A71E–04, 2002.

Nickovic, S.: Saharan dust outbreaks: modelling. First EARLINET symposium on the structure and use of the data base derived from systematic lidar observations, Hamburg, 11–12 February, 2003.

Nickovic, S.: Distribution of dust mass over particle sizes: impacts on atmospheric optics, Forth ADEC Workshop – Aeolian Dust Experiment on Climate Impact, Nagasaki, Japan, 357–360, 26–28 January, 2005.

Nickovic, S., Kallos, G., Papadopoulos, A., and Kakaliagou, O.: A model for prediction of desert dust cycle in the atmosphere, J. Geophys. Res., 106, 18113–18129, 2001.

Nickovic, S., Pejanovic, G., Ozsoy, E., Pérez C., and Baldasano, J. M.: Interactive Radiation-Dust Model: A Step to Further Improve Weather Forecasts. International Symposium on Sand and Dust Storm, Beijing, China, 12–14 September, 2004.

Nickovic, S., Vukovic, A., Vujadinovic, M., Djurdjevic, V., and Pejanovic, G.: Technical note: High-resolution mineralogical database of dust-productive soils for atmospheric dust modeling, Atmos. Chem. Phys., 12, 845–855, doi:10.5194/acp-12-845-2012, 2012.

Pauley, M. P., Baker, L. N., and Barker, H. E.: An observational Study of the “Interstate 5” Dust Storm Case. Bull. Amer. Meteor. Soc., 77, 693–720, 1996.

Pejanovic, G., Vukovic, A., Vujadinovic, M., and Dacic, M.: Assimilation of satellite information on mineral dust using dynamic re-

laxation approach, Geophys. Res. Abstracts, 12, EGU2010-7353, 2010.

Pérez, C., Nickovic, S., Baldasano, J., Sicard, M., Rocadenbosch, F., and Cachorro, V. E.: A long Saharan dust event over the western Mediterranean: Lidar, Sun photometer observations, and regional dust modeling, J. Geophys. Res., 111, D15214, doi:10.1029/2005JD006579, 2006.

Pérez, C., Haustein, K., Janjic, Z., Jorba, O., Huneeus, N., Baldasano, J. M., Black, T., Basart, S., Nickovic, S., Miller, R. L., Perlwitz, J. P., Schulz, M., and Thomson, M.: Atmospheric dust modeling from meso to global scales with the online NMMB/BSC-Dust model – Part 1: Model description, annual simulations and evaluation, Atmos. Chem. Phys., 11, 13001–13027, doi:10.5194/acp-11-13001-2011, 2011.

Prasad, A. K. and Singh, R. P.: Changes in aerosol parameters during major dust storm events (2001–2005) over the Indo-Gangetic basin using AERONET and MODIS data, J. Geophys. Res., 112, D09208, doi:10.1029/2006JD007778, 2007.

Prasad, A. K., Singh, R. P., and Singh, A.: Seasonal climatology of aerosol optical depth over Indian subcontinent: trend and departures in recent years, Int. J. Remote Sens., 27, 2323–2329, 2006.

Prasad, A. K., El-Askary, H., and Kafatos, M.: Implications of high altitude desert dust transport from Western Sahara to Nile Delta during biomass burning season, Environ. Pollut., 158, 3385–3391, 2010.

Prospero, J. M., Ginoux, P., Torres, O., Nicholson, S. E., and Gill, T. E.: Environmental characterization of global sources of atmospheric soil dust identified with the NIMBUS 7 Total Ozone Mapping Spectrometer (TOMS) absorbing aerosol product, Rev. Geophys., 40, 1002, doi:10.1029/2000RG000095, 2002.

Raman, A. and Arellano Jr., F. A.: Modeling and Data Analysis of 2011 Phoenix Dust Storm, 93rd AMS annual meeting, 5–10 January, Austin, Texas, 2013.

Rossa, A., Nurmi, P., and Ebert, E.: Overview of methods for the verification of quantitative precipitation forecasts, in: Precipitation: Advances in Measurement, Estimation and Prediction, edited by: Michaelides, S., Springer, Berlin, Germany, 417–450, 2008.

Ryzhkov, A. V., Schuur, R. J., Burgess, D. W., Heinselman, P. L., Giangrande, S. E., and Zrnic, D. S.: The Joint Polarization Experiment: Polarimetric rainfall measurements and hydrometeor classification. Bull. Amer. Meteor. Soc., 86, 809–824, 2005.

Schepanski, K., Flamant, C., Chaboureau, J.-P., Kocha, C., Banks, J., R., Brindley H. E., Lavaysse, C., Marnas, F., Pelon, J., and Tulet P.: Characterization of dust emission from alluvial sources using aircraft observations and high-resolution modeling, J. Geophys. Res., 118, 7237–7259, doi:10.1002/jgrd.50538, 2013.

Segal, M.: On the impact of thermal stability on some rough flow effects over mobile surfaces, Bound. Layer Meteorol., 52, 193-198, 1990.

Shao, Y. and Dong, C. H.: A review on East Asian dust storm climate, modeling and monitoring, Global Planet. Change, 52, 1–22, 2006.

Shirazi, M. A., Boersma, L., and Johnson, C. B.: Particle size distributions: Comparing texture systems, adding rock, and predicting soil properties, Soil Sci. Soc. Am. J., 65, 300–310, 2001.

Solomos, S., Kallos, G., Mavromatidis, E., and Kushta, J.: Density currents as a desert dust mobilization mechanism, Atmos. Chem. Phys., 12, 11199–11211, doi:10.5194/acp-12-11199-2012, 2012.

Sprigg, W. A., Barbaris, B., Morain, S., Budge, A., Hudspeth, W., and Pejanovic G.: Public Health Applications, Remote Sens., doi:10.1117/2.1200902.1488, 2008.

Sprigg, W. A., Galgiani, J. N., Nickovic, S., Pejanovic, G., Vujadinovic, M., Vukovic, A., Prasad, A., Petkovic, S., El-Askary, H., Gaddi, R., Janjic, Z., Pappagianis, D., Sarafoglou, N., Kafatos, M., Bruck M., and Ferng, M.-J.: Airborne Dust Models: A Tool in Environmental Health Tracking; final report, CDC, Atlanta, GA, 180 pp., 2012.

Sundram, I., Claiborn, C., Strand, T., Lamb, B., Chandler, D., and Saxton, K.: Numerical modeling of windblown dust in the Pacific Northwest with improved meteorology and dust emission models, J. Geophys. Res., 109, D24208, doi:10.1029/2004JD004794, 2004.

Sutton, L. J.: Haboobs, Q. J. Roy. Meteorol. Soc., 51, 25–30, 1925.

Sutton, L. J.: Haboobs, Q. J. Roy. Meteorol. Soc., 57, 143–162, doi:10.1002/qj.49705723906, 1931.

Tegen, I. and Lacis, A. A.: Modeling of particle size distribution and its influence on the radiative properties of mineral dust aerosol, J. Geophys. Res., 101, 19237–19244, doi:10.1029/95JD03610, 1996.

Tegen, I., Harrison, S. P., Kohfeld, K., Prentice, I. C., Coe, M., and Heimann, M.: Impact of vegetation and preferential source areas on global dust aerosol: Results from a model study, J. Geophys. Res., 107, 4576, doi:10.1029/2001JD000963, 2002.

Tegen, I., Schepanski, K., and Heinold, B.: Comparing two years of Saharan dust source activation obtained by regional modelling and satellite observations, Atmos. Chem. Phys., 13, 2381–2390, doi:10.5194/acp-13-2381-2013, 2013.

Todd, M. C., Karam, D. B., Cavazos, C., Bouet, C., Heinold, B., Baldasano, J. M., Cautenet, G., Koren, I., Pérez, C., Solmon, F., Tegen, I., Tulet, P., Washington, R., and Zakey, A.: Quantifying uncertainty in estimates of mineral dust flux: An intercomparison of model performance over the Bodele Depression, northern Chad, J. Geophys. Res.-Atmos., 113, D24107, doi:10.1029/2008JD010476, 2008.

Uno, I., Wang, Z., Chiba, M., Chun, Y. S., Gong, S. L., Hara, Y., Jung, E., Lee, S. S., Liu, M., Mikami, M., Music, S., Nickovic, S., Satake, S., Shao, Y., Song, Z., Sugimoto, N., Tanaka, T., and Westphal, D. L.: Dust model intercomparison (DMIP) study over Asia: Overview, J. Geophys. Res.-Atmos., 111, D12213, doi:10.1029/2005JD006575, 2006.

US Department of Agriculture: State soil geographic (STATSGO) data base-data use information, miscellaneous publication number 1492 (rev. ed.): Fort Worth, Texas, Natural Resources Conservation Service (variously paged), 1994.

Vukovic A., Pejanovic G., Vujadinovic M., Sprigg W., Nickovic S., and Djurdjevic V.: Dust storm of July 5^{th} 2011, Phoenix, Arizona: Numerical simulation, U14A-05, AGU Fall Meeting,San Francisco, California, USA, 5–9 December 2011.

Walker, A. L., Liu, M., Miller, S. D., Richardson, K. A., and Westphal, D. L.: Development of a dust source database for mesoscale forecasting in southwest Asia, J. Geophys. Res., 114, D18207, doi:10.1029/2008JD011541, 2009.

Wilkerson, D. W.: Dust and Sand Forecasting in Iraq and Adjoin Countries, Air Weather Service, Scott Air Force Base, Illinois, USA, 1991.

Winker, D. M., Hunt, W. H., and Hostetler, C. A.: Status and performance of the CALIOP lidar, Proc. SPIE-Int. Soc. Opt. Eng., 5575, 8–15, 2004.

Xie, J., Yang, C., Pejanovic, G., Nickovic, S., Zhou, B., and Huang Q.: Utilize multi CPU cores to improve dust simulation performance, Eos Trans. AGU, 89, Fall Meet. Suppl., Abstract: IN23C-1103, 2008.

Xu, D., Qu, J. J., Niu, S., and Hao, X.: Sand and dust storm detection over desert regions in China with MODIS measurements, Int. J. Remote Sens., 32, 9365–9373, 2011.

Yin, D., Nickovic, S., Barbaris, B., Chandy, B., and Sprigg, W. A.: Modeling wind-blown desert dust in the southwestern United States for public health warning: a case study, Atmos. Environ., 39, 6243–6254, doi:10.1016/j.atmosenv.2005.07.009, 2005.

Yin, D. and Sprigg, W. A.: Modeling Airbourne Mineral Dust: A Mexico – United States Trans-boundary Perspective, in: Southwestern Desert Resources, edited by: Halvorson, W., Schwalbe, C., and van Riper III, C., University of Arizona Press, Tucson, AZ, 303–317, 2010.

Zender, C. S., Newman, D., and Torres, O.: Spatial heterogeneity in aeolianerodibility: Uniform, topographic, geomorphic, and hydrologic hypotheses, J. Geophys. Res., 108, 4543, doi:10.1029/2002JD003039, 2003.

Zrnic, D. S. and Ryzhkov, A. V.: Polarimetric properties of chaff, J. Atmos. Ocean. Technol., 21, 1017–1024, 2004.